

Proceedings of the 35th European Safety and Reliability & the 33rd Society for Risk Analysis Europe Conference
 Edited by Eirik Bjorheim Abrahamsen, Terje Aven, Frederic Boudier, Roger Flage, Marja Ylönen
 ©2025 ESREL SRA-E 2025 Organizers. Published by Research Publishing, Singapore.
 doi: 10.3850/978-981-94-3281-3_ESREL-SRA-E2025-P8986-cd

Improvement of mountain natural risks analysis: assessment of reach, seasonal exposure and presence probabilities

Jean-Marc Tacnet

Univ. Grenoble Alpes, CNRS, INRAE, IRD, Grenoble INP, IGE, France. E-mail: jean-marc.tacnet@inrae.fr

Jean Dezert

ONERA, The French Aerospace Lab, France. E-mail: jdezert@gmail.com

Simon Carladous

Dir. risques naturels, ONF-RTM, ONERA, France. E-mail: simon.carladous@onf.fr

Christophe Bérenguer

*Univ. Grenoble Alpes, CNRS, Grenoble-INP, Gipsa-lab, France.
 E-mail: Christophe.Berenguer@gipsa-lab.grenoble-inp.fr*

Mountain natural phenomena threaten people and infrastructures. Risk-informed decision making to select risk reduction measures always starts with risk analysis. Natural risks are assessed through a combination of hazard, exposure and vulnerability (equivalent to severity and probability in industrial technological contexts). In practice, characterizing the exposure is indeed not that easy since for a given magnitude, a phenomenon can have several possible trajectories, each of them corresponding to a sub-scenario with a given conditional probability. Seasonal mountain phenomena occurrence and human touristic occupation are highly variable inducing peaks in occupancy rates. This paper addresses the issue of operational assessment of assets exposure considering their seasonal reach and presence probability for different phenomenon sub-scenarios. Simplified and practical methodologies are proposed to first calculate risk based on seasonal phenomenon occurrence and exposure and secondly calculate the reach probabilities of their spatial extent. Simple examples are given for a first single phenomenon (torrential flood) and demonstrate the influence of seasonal occurrence and presence hypothesis on calculated risks. Methodologies can be extended to deal with multi-risk contexts.

Keywords: mountain, natural risks, scenarios, risk analysis, exposure, reach probability, presence probability

1. Introduction

1.1. Risk components and required probabilities

Mountain natural phenomena such as torrential floods, snow avalanches, rockfalls threaten people, buildings and all kinds of critical infrastructures. To reduce risk, local authorities and infrastructures managers are searching for the best strategies and actions at local and also territorial scales. Spatialized risk analysis remains the first essential step for risk-informed decision making aiming to determine risk level and then choose the best risk reduction measures and strategies which include non-structural measures such as risk information, land use control, evacuation and alert plans and also structural measures such

as protective structures (Tacnet et al., 2014). Numerous risk equations and application cases of quantitative risk analysis (QRA) exist. Description and quantitative assessment of risk components are classical, well known processes including quantifying hazard, exposure and vulnerability (Kaplan et al., 2001; Farvacque et al., 2024; New, 2022). Combination of a danger's probability and related losses for a given type of asset are implemented with varying levels of detail and complexity. Operational, territorial risk assessment and management (i.e decision-making) processes require simple approaches. To be used in practice, we consider the following components used in a simplified risk equation in view of above existing QRA equations (Eq.(1)): \otimes an operator meaning

combination, *Scenario* \triangleq set of considered event scenarios S defined as triplets (p, o, ef) , each representing a phenomenon event p , its occurrence o and the considered effect ef ; *phenomenon* \triangleq set of considered phenomena p (torrential flood, snow avalanche ...); *Occur. proba.* \triangleq considered occurrence probability (or return period) O for a given effect of a phenomenon (e.g. 10, 100 years return period height of torrential floods; *effect* \triangleq considered physical effects ef of a given phenomenon scenario (e.g. submersion, impact, scouring for a torrential flooding phenomenon); *intensity* \triangleq intensity of each effect associated to a phenomenon scenario; *Elt* \triangleq set of all elements elt_i (assets, people ...) at risk; *expo* \triangleq representing the exposure (i.e. elements impacted by the phenomenon; *eltTypeNb* \triangleq number of elements at risk of a considered given type (e.g. number of a given type of building, infrastructures, number of people ...); *reach* \triangleq element at risk location's spatial reach probability (e.g. reach probability of a place where a building, a road, a powerplant ... is located, ; *pres* \triangleq element at risk presence probability (e.g. probability for a person to be inside a building reached by a phenomenon, for a vehicle to be inside an area reached by a phenomenon, note that presence probability can be different from 1 only for mobile elements or assets ; *capacity* \triangleq capacity (maximum number of persons inside an element at risk (e.g. max.number of persons inside a building, a vehicle); *occup.* \triangleq element at risk human occupancy probability (or rate), e.g. building, vehicle human occupation rate; *vul* \triangleq vulnerability (i.e. potential of damage of a given element at risk exposed to the effect of a phenomenon associated for a given intensity) ; *value* \triangleq value of the element at risk; *LOSS* \triangleq valuated damage of a given element at risk, equal to $LOSS = damage \otimes value$ with $damage = vul \otimes intensity$.

All the previous components are needed to calculate risk whatever the semantics which is used. Depending on contexts, this semantics may differ and those components may be gathered in different categories without any consequence on risk results (e.g. hazard, exposure, vulnerability for IPCC (New, 2022)). Note that we consider here

the description of assets as a part of exposure and the vulnerability term as a potential of damage for a given asset submitted to a given danger (see calculation example in Figure 5).

$$Risk = \sum_{Scenario} \sum_{Elt} \left(\begin{array}{c} \text{hazard} \\ \text{phenom.} \\ \otimes \text{effect} \\ \otimes \text{occu.} \\ \text{proba.} \\ \otimes \text{intensity} \end{array} \right) \otimes \left(\begin{array}{c} \text{LOSS} \\ \text{expo} \otimes \text{vul} \\ \text{eltTypeNb} \\ \otimes \text{reach} \\ \otimes \text{capacity} \\ \otimes \text{pres} \\ \otimes \text{occup.} \\ \otimes \text{value} \end{array} \right) \quad (1)$$

1.2. Seasonal features of risk

Seasonal monthly phenomenon occurrence and material or human assets' presence probabilities and consequently the resulting risk value may be very different from one month to another. Both phenomena and exposure can be considered as seasonal. Snow avalanches (e.g.) only occur during in winter while others such as floods, landslides, rockfalls may occur all year round. A constant mean annual event probability is generally considered in risk calculation even if the occurrence of some phenomena at a given period is known to be impossible. Risk value may therefore be correct from an annual point of view but it may not be representative of some peak risk period during the year. The same issue can be identified when dealing with exposure corresponding to exposed people and mobile assets (vehicles, seasonal buildings). Mountain are generally highly touristic areas and exposure levels may be increased for occupants of buildings or temporary accommodation, vehicles, their loads and passengers in areas affected by the phenomena. Occupancy rate, the road traffic can increase a lot during holidays periods. Road traffic to access the sites is also characterized by periods of heavy use, which can lead to congestion, potentially increasing the level of risk. Mean traffic values therefore do not capture peak exposure values. Presence probability at a given point and occupancy rates are therefore key risk components which should

be assessed.

1.3. Spatial features of risk

A phenomenon event (torrential flood, rockfall, snow avalanche) of a given magnitude and occurrence probability can propagate on a given area with different trajectories or extensions. For instance, a torrential debris-flows can overflow and impact houses far from the usual torrent axis while homes in the immediate vicinity of the torrent bank will not be affected. Each occurrence of the phenomenon is called an event scenario which can include several sub-scenarios, each of them having their own reaching spatial extension (Z_j) and a given intensity. For torrent flood sub-scenarios, functional failures can correspond to overflow extensions Z_j on the edge of main channel which can be caused either by an obstruction at a singularity (e.g. a bridge) or an exceeding hydraulic capacity on a channel section (Fig 2). Figure 1 shows two torrential flood overflow scenarios T_1 and T_2 with respective overlapping extensions Z_1 and Z_2 .

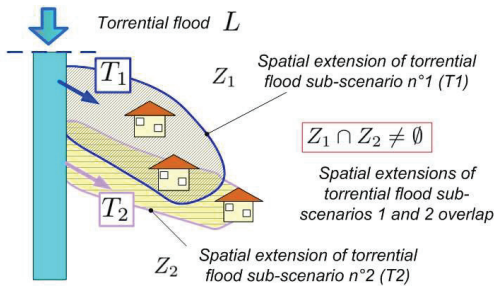


Fig. 1. Overlapping of the extensions of two torrential floods sub-scenarios T_1 and T_2 .

To analyze risk in the affected area, assessment of the reach probability at any point given the conditional probability of each sub-scenario and its spatial extension is needed.

1.4. Needs and objectives

This paper contributes to assess seasonal risk considering seasonal phenomenon occurrence, human and material assets' presence and occupancy and reach probabilities considering different phenomenon trajectories sub-scenarios (see Figure 2).

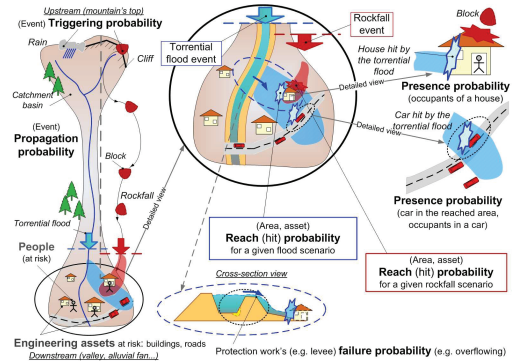


Fig. 2. Several probabilities are needed to assess (natural) risks.

First section presents the context, the objectives and recalls the main risk concepts. Section 2 recalls the underlying hypothesis assimilating the phenomenon occurrence process to a Poisson process and then justifies and describes the assessment of seasonal phenomenon occurrence, exposure and risk. Section 3 deals with the assessment of multi-scenarios spatial reach probability. Section 4 concludes the paper and presents perspectives.

2. Seasonal phenomenon occurrence, exposure and risk

Natural events' average return interval (ARI) and annual exceedance probability (for a given magnitude) (AEP) are classically determined using event time series through (e.g.) hydrological studies when dealing with floods (Musy, 2005). Frequency analysis of historical events aims fitting measured values to a probability law, such as Gumbel's law for annual maximums. This allows to determine, for rare events, the mean annual exceedance probability (AEP) linked to hazard magnitude levels (e.g. $P(Q \leq Q_{ref}) = 0.01$). In practice, once the reference average return interval ARI (e.g. 100 years) has been chosen for all the considered phenomena (e.g. floods, snow avalanches ...), its inverse is directly considered as $AEP = \frac{1}{ARI} = 0.01$. This classical operational practice is indeed based on an underlying (often not explicit) assimilation of the phenomenon occurrence process to a Poisson process.

In this section, we recall the theoretical foundations of calculations and transformation of *ARI* into *AEP* and the way, the Poisson process assumption also allows to calculate a seasonal phenomenon occurrence probability on a sub-period of a year knowing the mean annual value.

2.1. Considering phenomenon occurrence as a Poisson process

A Poisson process of intensity λ (strictly positive real, corresponding to a temporal occurrence) is an event occurrence counting process that verifies the three following conditions: 1) Numbers of occurrences in disjoint time intervals are independent; 2) The probability of an occurrence in a small time interval is proportional to the length of that interval, the proportionality coefficient being λ ; 3) The probability of more than one occurrence in a small time interval is negligible. The two last conditions 2 and 3 correspond to the so-called “rare events” property. If we note N_t the considered Poisson process with $t \in \mathbf{R}^+$ and P the probability, those properties can be formulated as: 1) $\forall t_0 = 0 \leq t_1 < \dots < t_k$, the random variables $(N_{t_k} - N_{t_{k-1}}), \dots, (N_{t_1} - N_{t_0})$ are independent; 2) $P(N_{t+h} - N_t = 1) = \lambda \cdot h + o(h)$ when $h \rightarrow 0^+$, t being fixed; 3) $P(N_{t+h} - N_t > 1) = o(h)$ when $h \rightarrow 0^+$, t being fixed. On these basis, we get $P(N_{t+h} - N_t = 0) = 1 - \lambda \cdot h + o(h)$. Property 2 means that, under the assumption of a constant annual event occurrence rate λ , small wrt. 1, the conditional probability of an event occurrence between t and $t + h$ knowing that it has not been observed at time t can be approximated by λh , whatever t . N_t , the number of event occurrences on a time interval t , follows a Poisson law with an intensity λ which gives : $P(N_t = k) = e^{-\lambda t} \cdot \frac{(\lambda t)^k}{k!}$ with k in \mathbb{N} . the random variables $S_k = T_k - T_{k-1}$ (time between two occurrences with k in \mathbb{N}^* are independent and $P(S_k \leq t) = 1 - e^{-\lambda t}$.

2.2. Average recurrence interval (ARI) and Annual Exceedance Probability (AEP)

System failures and phenomenon occurrences may both be modeled as Poisson processes, fea-

turing the similarity between natural risks and RAMS (Reliability, Availability, Maintainability and Security) contexts. Under this assumption, natural events’ and system failures’ occurrences are described using a constant annual rate denoted respectively by $\frac{1}{ARI}$ or λ but corresponding to the same concept.

ARI (years)	5	10	20	50	100	200
AEP (rigorous calculation)	0.1813	0.0952	0.0488	0.0198	0.0100	0.0050
Approximate calculation AEP=1/ARI	0.2	0.1	0.05	0.02	0.01	0.005
Overestimating error (simplified/rigorous)	10.33%	5.08%	2.52%	1.00%	0.50%	0.25%

Fig. 3. Comparison of approximate and rigorous calculation of *AEP* for different values of *ARI*.

Schmidt et al. (2011) (e.g.) applies the Poisson process assumption to natural hazard risk context without clearly recalling theoretical backgrounds. The average recurrence interval (*ARI*) is assimilated to the average, or expected, length of the time periods in years between hazard events whose magnitude exceeds a given threshold. A 10-years *ARI* implies that, on average, an event of the given size or larger will occur every ten years. The annual exceedance probability (*AEP*) is defined as the probability that a hazard event of a given magnitude or larger will occur in any one year. The relationship between *ARI* (year⁻¹) and *AEP* (in year) is

$$AEP = 1 - e^{-\left(\frac{1}{ARI}\right)t_1} \quad (2)$$

with $t_1 = 1$ year, which can be approximated by $AEP \simeq \left(\frac{1}{ARI}\right)t_1$ for *ARI* > 10 years. *AEP* is therefore linked to the process intensity λ with $AEP \simeq \left(\frac{1}{ARI}\right)t_1 = \lambda t_1$ and *ARI* is equivalent to a mean time between failure (*MTBF*) with $ARI = MTBF$. Underlying approximations are as follows: we have $e^x \simeq 1 + x + \frac{x^2}{2}$ for $x \ll 1$ and therefore $1 - e^{-\lambda t} = \lambda t + \frac{(\lambda t)^2}{2}$. The error done when approximating *AEP* by $\left(\frac{1}{ARI}\right)t_1$ can then be estimated as $\frac{\left(\left(\frac{1}{ARI}\right)t_1\right)^2}{2}$. Figure 3 calculates this error for different values of *ARI*.

We recall here a well known result. Non specialists may often consider that the probability P_{ARI} that a 100 years return period phenomenon

($ARI = 100$ years) occurs during 100 years equals to 1 while the correct value is approx. 0.63. Demonstration calculation of P_{ARI} is done as follows. Knowing ARI , we get $AEP = \frac{1}{ARI} \cdot t_1$ with $t_1 = 1$ year. The annual probability of non-exceedance equals $1 - AEP$. The probability of non-exceedance during n years is $(1 - AEP)^n$. Therefore $P_{ARI} = 1 - (1 - AEP)^{ARI}$. This value, calculated with approximation (P_{ARI1}) or exact value (P_{ARI2}) of AEP is compared with Eq.(2)) corresponding to the Poisson process definition (P_{ARI3}) (see Figure 4).

2.3. From mean annual to sub-periods failure probabilities

Knowing ARI and AEP on a year, our objective is to calculate $SPEP$ corresponding to the exceedance probability for the considered sub-period. Let us consider n sub-periods of a unit time whose duration equals to $1/n$ year. If the unit time is a year, $n = 12$ if the sub-period is a month ($n = 365$ if sub-period is a day). Sub-periods can correspond to real existing calendar sub-periods or to any part of a year. In Figure 6 (e.g.), we will consider only the 5 winter months. With the assumption of an underlying Poisson process, Property 2 described in Section 2.1 can be used to state directly that the occurrence probability on any sub-period $h = \frac{1}{n}$ year is equal to $\lambda_n = \frac{\lambda}{n}$. We consider a system where a natural phenomenon occurs (considered as a failure) every ARI years in average, the year being divided in n sub-periods. We search both AEP and the exceedance probability for each sub-period of the year ($SPEP$). Considering different approximations to calculate AEP , we determine the errors which are therefore done on AEP and $SPEP$ depending both on used method and value of ARI (see Figure 4). The annual exceedance probability (of failure) per year which equals to $AEP = \lambda \cdot t_1 = 1 - e^{-\left(\frac{1}{ARI}\right)t_1}$ is possibly approximated by $\left(\frac{1}{ARI}\right) \cdot t_1$ with $t_1 = 1$ year. The annual non-exceedance probability (no failure) is equal to $q = 1 - AEP$. With sub-periods, $P(X \leq 1) = 1 - (1 - P(X \leq \text{subperiod}))^n$ with X the date of occurrence. We have $P(X \leq \text{year}) = \lambda \cdot t$ and $P(X \leq \text{subperiod}) = \lambda_n \cdot t$. We have

therefore $\lambda = 1 - (1 - \lambda_n)^n$ which gives $\lambda_n = 1 - (1 - \lambda)^{\frac{1}{n}}$. Having justified the calculation process of $SPEP$, we analyze the effect of different approximation on $SPEP$ (and therefore on seasonal risk) depending on ARI values (Figure 4). Previous λ_n calculation is compared with a direct result considering that $\lambda_n = \frac{\lambda}{n}$. The approximation $AEP = \frac{1}{ARI} \cdot t_1$ induces less than 1% for $ARI \geq 30$ years (this suggests to be cautious for small ARI values (≤ 10 years)). The calculation consisting in considering $SPEP = \frac{1}{(ARI \cdot n)} \cdot t_1$ with $t_1 = 1$ year is also valid and can be used in seasonal risk assessment approaches. Approximations validity increases with ARI values and number of sub-periods. This is the direct consequence of the error made when approximating $1 - e^{-x}$ by x when x is too big wrt. 1. The greater the number of sub-periods, the better the result of AEP simply because $\lambda_n \cdot t_1$ becomes small wrt 1 (in sub-period unit) when the number of sub-periods increases.

ANNUAL				
ARI (in years)	5	10	30	100
Annual failure rate : lambda	0.2	0.1	0.03	0.01
(AEP1): Approx AEP = (1/ARI).t	0.2	0.1	0.03	0.01
(AEP2): Exact AEP=1-EXP(-(1/ARI).t)	1.8127E-01	9.5163E-02	3.2784E-02	9.9502E-03
Error AEP1 vs. AEP2	9.37%	4.84%	1.65%	0.50%
(P_ARI1): 1-(1-AEP)^ARI with approx AEP (see AEP1)	6.7232E-01	6.5132E-01	6.3834E-01	6.3397E-01
(P_ARI2): 1-(1-AEP)^ARI with exact AEP calculation (see AEP2, Eq.2)	6.3212E-01	6.3212E-01	6.3212E-01	6.3212E-01
(P_ARI3): 1-EXP(-(1/ARI).ARI)	6.3212E-01	6.3212E-01	6.3212E-01	6.3212E-01
Error P_ARI2 vs. P_ARI3	3.51E-16	3.51E-16	-3.51E-16	-1.41E-15
Error P_ARI1 vs. P_ARI2	6.4%	3.0%	1.0%	0.3%
Error P_ARI1 vs. P_ARI3	6.36%	3.04%	0.98%	0.29%
SUB-PERIODS				
n : number of subperiods in a year (e.g. months)	12	12	12	12
(SPEP1): approximate calculation SPEP=lambda_n.t=(lambda/n).t	1.6667E-02	8.3333E-03	2.7778E-03	8.3333E-04
(SPEP2): lambda_n=1-(1-lambda)^Y(1/n)	1.8423E-02	8.7416E-03	2.8211E-03	8.3718E-04
(SPEP3): exact Poisson SubPEP 1-(1-exactAEP)^Y(1/n)	1.6529E-02	8.2987E-03	2.7739E-03	8.3299E-04
Error SPEP1 vs. SPEP2	-9.54%	-4.67%	-1.54%	-0.46%
Error SPEP1 vs. SPEP3	0.84%	0.42%	0.14%	0.04%
Error SPEP2 vs. SPEP3	11.5%	5.3%	1.7%	0.5%
APRI : average period return interval =ARI n (nb. of subperiods)	60	120	360	1200
(SPEP1): approx SPEP= (1/(APRI)).t	1.6667E-02	8.3333E-03	2.7778E-03	8.3333E-04
(AIISPEP): exact subPEP (see Eq.2)	1.6529E-02	8.2987E-03	2.7739E-03	8.3299E-04
Error SPEP1 vs. AIISPEP	0.83%	0.42%	0.14%	0.04%

Fig. 4. Comparison of approximate and rigorous calculation of event sub-period (seasonal) probabilities.

2.4. Example of calculation of seasonal risk

We consider a medium intensity snow avalanche whose average return interval (ARI) is 10 years.

The approximate probability of failure per year is equal to $p = \lambda \cdot 1 = (\frac{1}{ART}) \cdot 1 = (\frac{1}{10}) \cdot 1$ (approximate calculation). We consider that 100 buildings are exposed. Avalanche occurrence probability is considered as constant not during all over the year but only during a part of the year, corresponding to $n = 5$ months of winter season. The probability equals to 0 for the remaining 7 months. (n is not always a strict real existing time division of a year).

Hazard	Annual	Nature of phenomenon		avalanche
		Intensity of the phenomenon		medium
Season		Avalanche average return interval (ARI) in years		10
		annual failure rate : λ_y		0.1
		Occur : Approximate mean Annual Exceedance Probability (AEP)		0.1
		Rigorous mean Annual Exceedance Probability		0.0952
		Number of subperiods/years (months)		12
		Number of sub-periods (during ARI)		120
		Monthly Exceedance Probability (MEP)		8.33E-04
		Number of (phenomenon) seasonal sub-periods		5
		Number of seasonal subperiods (during ARI)		50
		Mean sub-period avalanche exceedance probability		2.00E-03
Material exposure		ElTypeNb: Number of buildings		100
		Mean area of each building (m ²)		100
		Value : Unit value/m ² in euros		2000
		Reach probability of the asset		0.7
		Presence probability of the asset		1
		Vulnerability rate (for a medium intensity avalanche)		0.2
		Mean capacity for each building		8
		Number of occupancy sub-periods (months)		0
		Mean annual human presence rate		0.522
		Mean annual human occupancy rate		0.446
Human Exposure				
Damage, fatalities				
Risk				

Fig. 5. Risk calculation with different seasonal phenomenon occurrence and exposure scenarios

Occupancy and presence rate of inhabitants are either constant all over the year or different between low and high season (Figure 6). Annual and sub-period occurrence probabilities are calculated

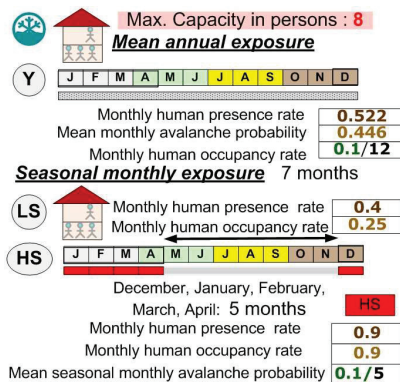


Fig. 6. Values of monthly mean annual and seasonal human presence and occupancy

as presented above and used to compare material and human risk values. Figure 5 shows the difference in calculated risk when considering only mean annual or seasonal occurrence and presence values.

3. Phenomenon scenarios, sub-scenarios and reach probabilities

3.1. Generic methodology for multi-scenarios spatial reach probability

We assume that the probability $P(L)$ of triggering and propagating the phenomena event L is known. We then consider N scenarios (i.e. possible extensions of torrential floods in the following example), denoted T_1, T_2, \dots, T_N . The trajectories are supposed to correspond to disjoint (i.e. exclusive) events which cannot occur simultaneously, i.e. their coexistence is impossible. We therefore have $0 \leq P(T_i|L) \leq 1$ and $\sum_{i=1}^N P(T_i|L) = 1$. We calculate the probability of being impacted by a natural phenomenon (say flood) called hit or reach probability, at a given point of a sub-area Z . The denomination of the reached zones A to G (Figure 8) were chosen has been chosen arbitrarily. It is more powerful to use a simpler automatic denomination (i.e. numbering) for a general implementation of probability calculation by the counting-method on a computer. For this automatic enumeration, we propose using the classic binary repre-

sensation on N bits^a with, by convention, the least significant bit on the right (LSBR). The position of the bit (from right to left) indicates the area entirely affected by the disaster trajectory. Bit no. 1 is the one furthest to the right of the binary code, since by convention the least significant bit is on the right. The second bit is the one to the left of the 1st bit, the 3rd bit is the one to the left of the 2nd bit, and so on. The first bit corresponds to the zone Z_1 , the 2nd bit to the zone Z_2 , and the 3rd bit to the zone Z_3 , and so on. Then we list the numbers from 1 to $2^N - 1$ with their associated binary representation. For example, if $N = 3$ (three affected areas as in figure 5), we will use the binary coding given in table shown on Figure 7. The last line of this table shows the fields corresponding to each column of the 3-bit binary code (or *binary word*). For any part numbered by the decimal value $n = 1, \dots, 2^N - 1$ (left-hand column of table shown on Figure 7), there is a unique N -bit binary code noted $(b_N(n), \dots, b_2(n), b_1(n))$ with $b_i(n) \in \{0, 1\}$. The value of the i th bit $b_i(n)$ of the binary code of part no n indicates whether this part n belongs to the Z_i zone when $b_i(n) = 1$, or not when $b_i(n) = 0$. According to this automatic numbering based on LSBR binary coding, part no. 1 belongs only to Z_1 , part no. 2 belongs only to Z_2 , part no. 3 belongs only to Z_1 and Z_2 but not to Z_3 , part no. 4 which belongs only to Z_3 , part no. 5 which belongs only to Z_1 and Z_3 but not to Z_2 , part no. 6 which belongs only to Z_2 and Z_3 but not to Z_1 , and part no. 7 which belongs to Z_1 , Z_2 and Z_3 . This corresponds to the numbering shown on the left side of Figure 7. This principle of automatically numbering the parts of affected sets/zones applies to any conceivable number $N > 3$ of impacted zones, and the counting-method can be applied to calculate automatically the probability to be impacted at a location z of any zone of surveillance, including multi-risk contexts. The reach probability can be used for risk calculation if the considered zones correspond to the same phenomenon intensity: the analysis must be done for each intensity level.

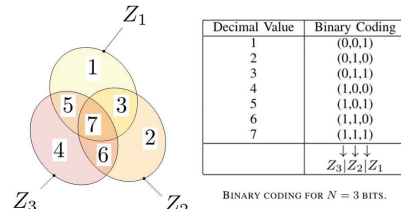


Fig. 7. Zones Z_1 , Z_2 and Z_3 with automatic part numbering.

3.2. Application to three torrential floods sub-scenarios

The methodology is applied to a torrential flood scenario composed of three trajectories sub-scenarios. We consider three overlapping trajectories T_1 , T_2 and T_3 for the torrential flood L (Figure 8) and the probabilities are given (by statistical analysis or experts assessments) : (e.g.) $P(T_1|L) = 0.50$, $P(T_2|L) = 0.30$ and $P(T_3|L) = 0.20$ checking that $P(T_1|L) + P(T_2|L) + P(T_3|L) = 1$. Seven zones named 1 to 7 can be identified (Figure 9). We are searching the reach probability of each of them. This means (if we simulate the phenomenon) that in 50% of cases we will get the impact in zone Z_1 , in 30% of cases we will get the impact in zone Z_2 and in 20% of cases we will get the impact in zone Z_3 . Over 10 draws, we will therefore have the following results^b:

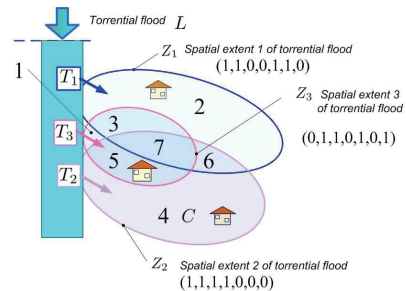


Fig. 8. Overlapping of three torrential floods extents.

For applying the counting-method we use the following 7-uples binary coding of the zones:

^a N is the number of impacted zones by each possible trajectory of the disaster.

^bThe order of the lines in Figure 9 is of no importance; we have indicated them in this way for the sake of presentation.

$Z_1 = (1, 0, 1, 0, 1, 0, 1)$ (Z_1 is composed of zones 1,3,5,7), $Z_2 = (1, 1, 0, 0, 1, 1, 0)$ (Z_2 is composed of zones 2,3,6,7) and $Z_3 = (1, 1, 1, 1, 0, 0, 0)$ (Z_3 is composed of zones 4,5,6,7) and we generate the counting-table given in Figure 9. By counting the occurrences of events (value 1) listed in Figure 9) for each zone from 1 to 7, we directly obtain the probabilities we want. We therefore get: $P(z \in 1|L) = 5/10 = 0.5$, $P(z \in 2|L) = 3/10 = 0.3$, $P(z \in 3|L) = 8/10 = 0.8$, $P(z \in 4|L) = 2/10 = 0.2$, $P(z \in 5|L) = 7/10 = 0.7$, $P(z \in 6|L) = 5/10 = 0.5$, $P(z \in 7|L) = 10/10 = 1$.

Path draws	(7, 6, 5, 4, 3, 2, 1)
T_1, Z_1	(1, 0, 1, 0, 1, 0, 1)
T_1, Z_1	(1, 0, 1, 0, 1, 0, 1)
T_1, Z_1	(1, 0, 1, 0, 1, 0, 1)
T_1, Z_1	(1, 0, 1, 0, 1, 0, 1)
T_1, Z_1	(1, 0, 1, 0, 1, 0, 1)
T_2, Z_2	(1, 1, 0, 0, 1, 1, 0)
T_2, Z_2	(1, 1, 0, 0, 1, 1, 0)
T_2, Z_2	(1, 1, 0, 0, 1, 1, 0)
T_3, Z_3	(1, 1, 1, 1, 0, 0, 0)
T_3, Z_3	(1, 1, 1, 1, 0, 0, 0)

Fig. 9. Simulation of the trajectories of disaster by random draws for 3 floods.

4. Discussion - Conclusion

Calculation of exceedance probability of year sub-periods is demonstrated and justified, which allows to use results to assess seasonal phenomenon occurrence and risk considering also seasonal exposure. The influence of seasonal features of occurrence and exposure is shown on a simple risk calculation example. An easy-to-use methodology is proposed to assess spatial reach probability on any point touched by different sub-scenarios trajectories corresponding to the same intensity of a given phenomenon event scenario. Available full theoretical probabilistic justifications of reach probability calculations were not provided. Others developments estimate sub-scenarios conditional probabilities and extend the approach to a multi-risk context. The reach probability depends on protection works' state and will evolve over time (Figure 2). Characterizing protection works' efficacy and the effect of their degradation

on downstream risk level are therefore additional key research topics for territorial risk management Carladous et al. (2019) and maintenance decision-making Chahrour et al. (2021) related to critical infrastructures.

Acknowledgement

This work has partially been done with support of the french Ministry of Ecology within the development of the STePRiM (Territorial strategy for mountain risk prevention) framework.

References

- Carladous, S., J.-M. Tacnet, M. Batton-Hubert, J. Dezert, and O. Marco (2019). Managing protection in torrential mountain watersheds: A new conceptual integrated decision-aiding framework. *Land Use Policy* 80, 464 – 479.
- Chahrour, N., M. Nasr, J. M. Tacnet, and C. Berenguer (2021). Deterioration modeling and maintenance assessment using physics-informed stochastic petri nets: Application to torrent protection structures. *Reliability Engineering and System Safety* 210.
- Farvacque, M., N. Eckert, G. Candia, F. Bourrier, C. Corona, and D. Toe (2024). Holistic rockfall risk assessment in high mountain areas affected by seismic activity: Application to the uspillata valley, central andes, chile. *Risk Analysis* 44(5), 1021–1045.
- Kaplan, S., Y. Haimes, and B. Garrick (2001). Fitting hierarchical holographic modeling into the theory of scenario structuring and a resulting refinement to the quantitative definition of risk. *Risk Analysis* 21(5), 807.
- Musy, A. (2005). Hydrologie générale - ecole polytechnique fédérale de lausanne. Technical report, Ecole Polytechnique Fédérale de Lausanne.
- New, M. e. a. (2022). Decision-making options for managing risk, chapter 17 in Pörtner H.-O. et al.(eds.), *Climate Change 2022: Impacts, Adaptation and Vulnerability. AR6 report*, Cambridge University Press, Cambridge, UK and New York, NY, USA, 2022. Technical report, IPCC.
- Schmidt, J., I. Matcham, S. Reese, A. King, R. Bell, R. Henderson, G. Smart, J. Cousins, W. Smith, and D. Heron (2011). Quantitative multi-risk analysis for natural hazards: A framework for multi-risk modelling. *Natural Hazards* 58(3), 1169 –1192.
- Tacnet, J.-M., J. Dezert, C. Curt, M. Batton-Hubert, and E. Chojnacki (2014, January 2014). How to manage natural risks in mountain areas in a context of imperfect information? new frameworks and paradigms for expert assessments and decision-making. *Environment Systems and Decisions* 34(2), 288–311.